Articles in PresS. Am J Physiol Gastrointest Liver Physiol (May 5, 2016). doi:10.1152/ajpgi.00035.2016

Transcriptomic and CRISPR/Cas9 technologies reveal FOXA2 as a tumor suppressor gene in pancreatic cancer.

Christina Vorvis[1], Maria Hatziapostolou[2], Swapna Mahurkar-Joshi[1], Marina Koutsioumpa[1], Jennifer Williams[3], Timothy R. Donahue[3], George A. Poultsides[4], Guido Eibl[3], Dimitrios Iliopoulos[1,#]

[1]Center for Systems Biomedicine, Division of Digestive Diseases, David Geffen School of Medicine, UCLA, Los Angeles, CA; [2]Centre for Biological Sciences, University of Southampton, Southampton, United Kingdom. [3]Department of Surgery, David Geffen School of Medicine, UCLA, Los Angeles, CA; [4]Department of Surgery, Stanford University School of Medicine, Stanford, CA;

Short title: FOXA2 as a tumor suppressor in pancreatic cancer

[#]Corresponding author:
Dimitrios Iliopoulos, PhD MBA, Center for Systems Biomedicine, Division of Digestive Diseases, David Geffen School of Medicine, UCLA, 650 Charles E. Young Dr., CHS 44-133, Los Angeles, CA 90095-7278

Copyright © 2016 by the American Physiological Society.

Abstract

Pancreatic ductal adenocarcinoma (PDAC) is a very aggressive cancer, with low survival rates and limited therapeutic options. Thus, the elucidation of signaling pathways involved in PDAC pathogenesis is essential to identify novel potential therapeutic gene targets. Here, we used a systems approach by integrating gene and microRNA profiling analyses together with CRISPR/Cas9 technology, to identify novel transcription factors involved in PDAC pathogenesis. FOXA2 transcription factor was found to be significantly down-regulated in PDAC relative to control pancreatic tissues. Functional experiments revealed that FOXA2 has a tumor suppressor function through inhibition of pancreatic cancer cell growth, migration, invasion and colony formation. *In situ* hybridization analysis revealed miR-199a significantly upregulated in pancreatic cancer. Bioinformatics and luciferase analyses showed that miR-199a negatively regulates directly FOXA2 expression, through binding in its 3' untranslated region (UTR). Evaluation of the functional importance of miR-199 on pancreatic cancer revealed that miR-199 acts as an inhibitor of FOXA2 expression, inducing an increase in pancreatic cancer cell proliferation, migration and invasion. Additionally, gene ontology and network analyses in PANC-1 cells treated with an siRNA against FOXA2 revealed an enrichment for cell invasion mechanisms through PLAUR and ERK activation. FOXA2 deletion (FOXA2Δ) by using two CRISPR/Cas9 vectors in PANC-1 cells, induced tumor growth *in vivo*, resulting in up-regulation of PLAUR and ERK pathways in FOXA2Δ xenograft tumors. Taken together, we have identified FOXA2 as a novel tumor suppressor in pancreatic cancer, regulated directly by miR-199a, enhancing our understanding on how microRNAs interplay with the transcription factors to affect pancreatic oncogenesis.

Keywords: FOXA2, miR-199a, CRISPR/Cas9, pancreatic cancer

Introduction

Pancreatic ductal adenocarcinoma (PDAC) accounts for >85% of all the pancreatic cancer cases. For all stages combined, the 1- and 5-year relative survival rates are 28% and 7%, respectively. More than half of patients (53%) are diagnosed at a late stage, where the 1- and 5-year survival rates reach 15% and 2%, respectively (44). Recently there are significant advances in the development of novel therapeutics, based on the rational design of targeted therapies directed at molecular alterations arising in cancer cells (72); however, PDAC remains a lethal disease. Even gemcitabine, the current standard of care chemotherapeutic, produces only a modest increase in survival in patients with PDAC (9). For metastatic disease, the standard of care is a combination four chemotherapeutic drugs, known as FOLFIRINOX (Folinic Acid, Fluorouracil, Irinotecan Hydrochloride, Oxaliplatin) (62). These treatments have limited efficacy and significant side effects, often only marginally improving the quality of life of patients (63). Therefore, there is an urgent need to identify novel therapeutic target molecules that a play a key role in pancreatic oncogenesis.

Premalignant lesions, known as pancreatic intraepithelial neoplasms (PanINs) are of ductal origin (32) and are thought to be precursors of ductal adenocarcinoma, as they progress toward increasingly atypical histological stages (40, 51, 55, 68). Multiple combinations of genetic mutations are commonly found in pancreatic adenocarcinomas (64). The *KRAS* gene, located on chromosome 12p, is one of the most frequently mutated genes in pancreatic cancer. The vast majority of mutations in this gene are at codon 12, leading to activation of the protein product of KRAS (33). *KRAS* mutations appear to occur very early in pancreatic carcinogenesis, indicating an important role in early initiation of disease (2). In addition to activating mutations, loss of function mutations in tumor suppressor genes is also commonly observed in pancreatic carcinomas. Loss of function occurs via inactivation mutations, homozygous deletions or DNA hypermethylation of the promoter areas of tumor suppressor genes, including *p16/CDKN2A,*

TP53, and SMAD4 that are inactivated in more than 50% of all pancreatic cancers (1, 30, 31, 58). Other pathways, involved in PDAC include, the Notch signaling pathway (Abel, 2014), the beta-catenin signaling pathway (46) and the PI3K/AKT signaling pathway (7). Although the role of different protein signaling pathways has been examined in pancreatic oncogenesis, the role and function of several transcription factor families has not been evaluated extensively.

Transcription factors affect downstream gene transcription of signal transduction pathways triggered by genetic and epigenetic changes linked to the aggressive nature of cancer (60). For example, the constitutive activation of NF-κB, which regulates the genes involved in many cellular processes, has also been implicated in the aggressive nature of PDAC (20). Signal transducer and activator of transcription 3 (STAT3) is activated in primary pancreatic cancer and is involved in various physiologic functions, including apoptosis, cell cycle regulation, angiogenesis, and metastasis (12). Negative regulation of STAT3 at the posttranscriptional level leads to attenuation of cell proliferation and invasion of pancreatic carcinoma (69), highlighting the importance of understanding transcriptional regulation in pancreatic oncogenesis. In 2012, Xia et al. identified a transcription factor, Forkhead Box M1 (FOXM1) that is associated with poor prognosis and could be used as a prognostic molecular marker and therapeutic target for pancreatic cancer (66).

In the present study, we sought to identify key transcriptional regulators that play a functional role in the pathogenesis of pancreatic cancer by performing transcription factor expression profiling followed by functional characterization of selected transcription factor. The aberrant expression of hepatocyte nuclear factor family of transcription factors (HNF1, HNF3, HNF4 and HNF6) have been implicated in a variety of solid tumors including lung, colorectal, hepatocellular and ovarian carcinoma (25, 43, 45, 49, 50, 73). The least studied hepatocyte nuclear factor gene family in cancer is HNF3. The hepatocyte nuclear factor 3 gene family encodes three transcription factors (HNF-3α, HNF-3β, and HNF-3γ) important in the regulation

of gene expression in normal liver and lung tissue, and were first identified by their ability to bind to important promoter elements in the α_1-antitrypsin and transthyretin genes (13). Our molecular and functional analysis revealed that HNF-3β, also known as forkhead box protein A2 (FOXA2), acts as a tumor suppressor gene in pancreatic cancer by affecting pancreatic cancer cell proliferation and invasiveness through regulation of urokinase plasminogen activator surface receptor (PLAUR) gene. Furthermore, we found that FOXA2 expression is regulated directly by miR-199, while inhibition of FOXA2 expression by using the CRISPR/Cas9 (*c*lustered *r*egularly *i*nterspaced *s*hort *p*alindromic *r*epeats-CRISPR associated nuclease 9) technology increases tumor growth in pancreatic tumor xenografts. Taken together, our study revealed a novel microRNA-transcription factor signaling pathway involved in the pathogenesis of pancreatic oncogenesis.

MATERIALS AND METHODS

Cell Culture

Human pancreatic cancer cell lines (AsPc-1, BxPC-3, Capan-1, Capan-2, HPAF-II and MIA PaCa-2, PANC-1) were purchased from ATCC. Human pancreatic cancer cell line PANC-1 was maintained in DMEM medium (Gibco) supplemented with 10% FBS and 10 units/ml penicillin, and 100 μg/ml streptomycin. AsPC-1 and BxPC-3 were maintained in RPMI-1640 medium (Gibco) supplemented with 10%FBS and 10 units/ml penicillin and 100 μg/ml streptomycin. Capan-1 was maintained in ATCC-formulated Iscove's Modified Dulbecco's Medium supplemented with 10% FBS and 10 units/ml penicillin and 100 μg/ml streptomycin. Capan-2 was maintained in ATCC-formulated McCoy's 5a Medium Modified supplemented with 10% FBS and 10 units/ml penicillin and 100 μg/ml streptomycin. HPAF-II was maintained in Eagle's Minimum Essential Medium with 10% FBS and 10 units/ml penicillin and 100 μg/ml streptomycin. MIA PaCa-2 was maintained in DMEM medium (Gibco) supplemented with 10%

FBS, horse serum to a final concentration of 2.5% and 10 units/ml penicillin and 100 μg/ml streptomycin.

RNA from PDAC and control samples

Human pancreatic tissues were obtained from consenting patients in the Department of Surgery at Stanford University and approved by the Ethics Committee of the Stanford University Medical School. RNA was extracted from 8 control (adjacent non-tumor) and 14 PDAC tissues using the TRIzol Reagent (15596-018, Life Technologies) RNA isolation method and were used for gene profiling. Nineteen control and 17 PDAC tissues were obtained from consenting patients in the Department of Surgery at the University of California, Los Angeles and approved by the UCLA Ethics Committee and were used to confirm gene expression array data.

Transcription factor expression analysis

To identify transcription factors that were differentially expressed in pancreatic ductal adenocarcinoma, microarray was performed using GeneChip® Human Genome U133 Plus 2.0 Arrays. RNA was isolated from 14 PDAC and 8 control tissues. In the list of top differentially expressed genes, FOXA2 was found to be down-regulated in PDAC (cut off was 2-fold change, $p<0.05$).

Invasion Assays

We performed invasion assays in PANC-1 and HPAF-II cells at 24 hours under different transfection conditions with siRNAs or microRNAs for 24 hours. Invasion of matrigel was conducted using standardized conditions with BD BioCoat Matrigel invasion chambers (BD Biosciences). Assays were conducted according to manufacturer's protocol, using 10% FBS as the chemoattractant. Non-invading cells on the top side of the membrane were removed, while invading cells were fixed and stained with 0.1 % crystal violet, 16 hours post-seeding. The cells that invaded through the filter were quantified by counting the entire area of each filter, using a grid and an Optech microscope at a 20X magnification. The experiment was repeated three times and the statistical significance was calculated using Student's t-test.

Migration Assays

PANC-1 and BxPC-3 pancreatic cancer cell lines were used in this assay. The migration assay was performed by starving cells overnight in media containing 0% FBS. The next day, cells were re-suspended in media with 0.5% FBS to a concentration of 5×10^5/ml. The upper chamber was loaded with 100 μL of cell suspension and the lower chamber was loaded with 500 μL medium containing 20% FBS as a chemoattractant. The cells on the bottom of each chamber were fixed with 0.1% glutaraldehyde for 30 min, rinsed briefly with PBS and stained with 0.2% crystal violet. The number of migrated cells was calculated using 20X magnification and the mean for each chamber was determined. The results were calculated as the migration rate as compared with the siRNA negative control (or miRNA-NC) cells. Each experimental condition was conducted in triplicates and the experiment was repeated three times.

Colony Formation Assays

PANC-1 cells were transfected with siRNA negative control or siFOXA2#2 for 48 hours. Triplicate samples of 10^5 cells from each cell line were mixed 4:1 (v/v) with 2.0% agarose in growth medium for a final concentration of 0.4% agarose. The cell mixture was plated on top of a solidified layer of 0.8% agarose in growth medium. Cells were fed every six to seven days with growth medium containing 0.4% agarose. The number of colonies was counted after 20 days. The experiment was repeated three times and the statistical significance was calculated using the Student's t-test.

In situ hybridization

Double-DIG labeled Mircury LNA probes were used for the detection of hsa-miR-199a-3p (38481-15, Exiqon) with target sequence ACAGUAGUCUGCACAUUGGUUA. *In situ* hybridization protocol was used as previously described (Iliopoulos et al., 2009b) with modifications. FFPE sections of control pancreatic and PDAC were deparaffinized with xylene (3x5 min), followed by treatment with serial dilutions of ethanol (3x100%, 2x96% and 3x70%) and by two changes of DEPC-PBS. Tissues were then digested with proteinase K (15 μg/ml) for 20 min at 37ºC, rinsed with 3xDEPC-PBS. Sections were dehydrated with 3x70%, 2x96% and 2x100% ethanol, air-dried and hybridized for 1 hour with the hsa-miR-199 probe (40nM) or the

double-DIG labeled U6 Control Probe (1nM) (99002-15, Exiqon) diluted in microRNA ISH buffer (90000, Exiqon) at 52ºC and 53 ºC, respectively. Following hybridization, sections were rinsed twice with 5XSSC, 2x1XSSC and 3x0.2XSSC, 5 min each, at 52ºC and PBS. The slides were incubated with blocking solution (11585762001, Roche) for 15 min and then with anti-DIG antibody (1:800) in 2% sheep serum (013-000-121, Jackson Immunoresearch) blocking solution for 1 hour at room temperature. Following three washes with PBS, 0.1% Tween-20, slides were incubated with the AP substrate buffer (NBT-BCIP tablet [11697471001, Roche] in 10 ml of 0.2mM Levamisole [31742, Fluka]) for 2 hours at 30ºC in the dark. The reaction was stopped with 2 washes of AP stop solution (50mM Tris-HCL, 150mM NaCl, 10mM KCl) and 2 washes with water. Tissues were counter stained with Nuclear Fast Red for 1 min and rinsed with water. Sections were dehydrated with 2x70%, 2x96% and 2x100% ethanol and mounted with coverslips in Eukitt mounting medium (361894G, VWR). Images were captured with a Nikon 80i Upright Microscope equipped with a Nikon Digital Sight DS-Fi1 color camera, using the NIS-Elements image acquisition software. All images were captured and processed using identical settings.

Immunohistochemistry

A pancreas disease spectrum tissue microarray of 103 cases was used (PA2081a, US Biomax, Inc.) containing 42 cases of pancreatic duct adenocarcinoma, three pancreatic adenosquamous carcinoma, one pancreatic islet cell carcinoma, six pancreatic metastatic carcinoma, 10 pancreatic islet cell tumor, 11 pancreatic inflammation and 21 adjacent normal pancreatic tissue, duplicated cores per case. Immunohistochemical staining for FOXA2 in control and pancreatic PDACs were deparaffinized with xylene (3x5 min) followed by treatment with serial dilutions of ethanol (100%, 100%, 95% and 95%, 10 min each) and by two changes of ddH2O. Antigen unmasking was achieved by boiling the slides (95-99ºC) for 10 min, in 10 mM sodium citrate, pH 6.0. Sections were rinsed three times with ddH2O, immersed in 3% H_2O_2 for 20 minutes, washed twice with ddH2O and once with TBS-T (TBS, 0.1% Tween-20) and blocked for 1 hour with blocking solution (5% normal goat serum [5425] in TBS-T). FOXA2 (sc-6554, Santa Cruz Biotechnology) antibody was diluted 1:250 in Signal Stain antibody diluent (8112, Cell Signaling Technology) and incubated with the sections overnight at 4ºC. Staining for mouse FOXA2, antibody was diluted 1:1000 in Signal Stain antibody diluent (sc-101060 Santa Cruz Biotechnology) and incubated with the sections overnight at 4ºC. Following incubation with the

antibody, sections were washed three times, 5 minutes each, with TBS-T and incubated for 1 hour at room temperature with SignalStain Boost ([HRP, Rabbit] 8114, Cell Signaling). Sections were washed three times, 5 minutes 22 each, with TBS-T, and stained with the DAB Peroxidase Substrate Kit (SK-4100, Vector Laboratories) for 30 minutes, washed and counterstained with the hematoxylin QS (H-3404, Vector Laboratories). Finally, tissues were dehydrated and mounted in Eukitt medium. Images were captured with a Nikon 80i Upright Microscope equipped with a Nikon Digital Sight DS-Fi1 color camera, using the NIS-Elements image acquisition software. All images were captured and processed using identical settings.

Real-Time PCR analysis

Quantitative real-time RT-PCR was performed to determine the expression levels of FOXA2 in 17 human PDAC tissues and 19 pancreatic control tissues for detection of miR-199a-3p. RNA was isolated using TRIzol, according to manufacturer's instructions (15596-018, Life Technologies). Real-time RT-PCR was assessed on a CFX384 detection system (BioRad) using the Exiqon PCR primer sets according to manufacturer's instructions. MicroRNA expression levels of miR-199 (204536, Exiqon) were normalized to the levels of U6 small nuclear snRNA (203907, Exiqon) and 5S rRNA (203906, Exiqon). Reverse transcription was carried out using the Universal cDNA synthesis kit (203301, Exiqon) and ExiLENT SYBR Green for RT-PCR (203403, Exiqon). Normalized miRNA levels were quantified relative to the levels of a given control tissue. Real-time PCR was employed to determine the expression levels of FOXA2 and PLAUR. Reverse transcription was carried out using iScript cDNA synthesis Kit (1708890, Bio-Rad). Real-time PCR was carried out using the iQ SYBR Green Supermix (1708882, Bio-Rad). Gene expression levels were normalized to the levels of Glyceraldehyde-3-phosphate dehydrogenase (GAPDH) and β-actin. Normalized gene expression levels were quantified to the respective control. The sequences of the primers used are the following:

FOXA2-F: 5'-ATGCACTCGGCTTCCAGTAT-3'

FOXA2-R: 5'-GTTGCTCACGGAGGAGTAGC-3'

PLAUR-F: 5'-GCATTTCCTGTGGCTCATC-3'

PLAUR-R: 5'- CTTTGGACGCCCTTCTTCA-3'

E-Cadherin-F: 5'-GGATTGCAAATTCCTGCCATTC-3'

E-Cadherin-R: 5'-AACGTTGTCCCGGGTGTCA-3'

GAPDH-F: 5'-ATGTTCGTCATGGGTGTGAA-3'

GAPDH-R: 5'-GGTGCTAAGCAGTTGGTGGT-3'

β-actin-F: 5'-CCCAGCACAATGAAGATCAA-3'

β-actin-R: 5'-ACATCTGCTGGAAGGTGGAC-3'

IL6-F: 5'- CTCTGGGAAATCGTGGAAATGAG -3'

IL6-R: 5'-CTGTATCTCTCTGAAGGACTCTG-3'

Luciferase Assay

MIA PaCa-2 cells were transfected with the reporter vectors carrying the 3′UTR of FOXA2 (S805635, SwitchGear Genomics. The constructs harbored the seed sequence of miR-199a-3p (wildtype) or had a mutation of this sequence (miR-199 mutant). At 24 hours, the cells were transfected with miR-negative control or miR-199 mimic and at 48 h luciferase activity was measured using the Dual Luciferase Reporter Assay System (E1910, Promega).

Cell growth Assays

PANC-1 and BxPC-3 pancreatic cancer cell lines were transfected with siFOXA2#2 or miR-199 mimic and their respective control and plated on a 96-well plate (5×10^2cells/well). Cell growth was assessed using the Cell-Titer Glo Luminescence Cell Viability Assay (G7571, Promega). The xCELLigence RTCA SP system utilizes a 96-well microtiter detection device, where the microelectrode sensor arrays are coated in 96-well microtiter plates and the microtiter plate detection device is connected to the workstation from the inside of the cell incubator. The impedance data from the selected well is exported to the computer and analyzed using RTCA software. A parameter termed cell index is used to quantify cell status based on detected cell-electrode impedance. Cell attachment and proliferation from selected wells of the plate were monitored and recovered every 15 minutes using the RTCA SP for 120h. The PANC-1 cells were transfected with miR-NC or miR-199. 24 hours post-transfection, cells were trypsinized

and cells were re-suspended at 5×10^3 cells/100 μL and 5×10^3 cells were seeded into each well of the E-plate 96 in quadruplicates.

Mouse experiments

$5x10^6$ PANC-1 control or PANC-1 FOXA2Δ cells were injected subcutaneously in the right flank of NOD/SCID mice (n= 10 mice/group). Tumor growth was monitored every seven days for a total period of 64 days. Tumor volumes were calculated by the equation V (mm^3) = $axb^2/2$, where "a" is the largest diameter and b is the perpendicular diameter. In addition, paraffin embedded tissue sections from pancreatic tissues from male 3-month and 9-month old, male, KrasG12D$^{+/-}$p48-Cre$^{+/-}$ (KC) mice, were provided by Dr. Guido Eibl's laboratory (15). All the mouse studies were approved by the University of California Institutional Animal Care and Use Committee and conformed to the US National Institutes of Health Guide for the Care and Use of Laboratory Animals.

Western blot analysis

Protein samples were subjected to SDS PAGE and transferred to polyvinylidene difluoride membranes in 25 mM Tris, 192 mM glycine. Membranes were blocked with 5% nonfat dry milk in PBS, 0.05% Tween-20 and probed with antibodies (1:1000) followed by corresponding horseradish peroxidase-labeled secondary antibodies (1:1000). Blots were developed with ECL reagent (T) and exposed in Eastman Kodak Co. 440 Image Station.

Antibodies and reagents

<u>Antibodies</u>

Two different antibodies against FOXA2 were used. One was used for western blotting experiments (8189, Cell Signaling) and the other (sc-6554, Santa Cruz Biotechnology) for immunohistochemical analysis. PLAUR antibody was used for western blotting experiments (9692, Cell Signaling). Additionally, phospho-p44/42 MAPK (Erk1/2)(Thr202/Tyr204) was used for western blotting in PANC-1 and HPAF –II cell lines (4370, Cell Signaling) along with total ERK antibody (4695, Cell Signaling), as well as total AKT (4691S, Cell Signaling) and phospho-AKT T308 (13038S, Cell Signaling) and phosphor-AKT S473 (4060S, Cell Signaling).

Additionally, CREB and GAPDH antibodies were used as loading controls (9104, Cell Signaling and 5174, Cell Signaling, respectively).

Small interfering RNAs

The following siRNAs were used in this study: siRNA negative control (siNC #2, 4390847, Life Technologies) and two different siRNAs against FOXA2 (siFOXA2#1, s6691, Life Technologies) and (siFOXA2#2, s6692, Life Technologies). A single siRNA against PLAUR was siPLAUR used in this study (s10614, Life Technologies).

FOXA2 Overexpression Vector

MiaPaCa-2 cells were transfected with vector plasmids as controls (Origene, PS100001) or plasmids for overexpression of FOXA2 (Origene, RC211408) according to manufacturer's protocol.

MicroRNAs

The following microRNAs were used in this study: *miR*Vana miRNA mimic, negative control #1 (miRNC, 4464059, Life Technologies) and miR-199 *miR*Vana miRNA mimic (4464066 miRVana miRNA mimic, Life Technologies).

3'UTR FOXA2 Vector

pLightSwitch_3UTR for FOXA was purchased from SwitchGear Genomics (S805635, SwitchGear Genomics), containing the miR-199a-3p predicted binding site.

CRISPR/Cas9 system

The FOXA2 human gene knockout kit via CRISPR was ordered from OriGene (KN204066). Clones were selected using 2µg/ml puromycin.

Statistical Analysis

All experiments were performed in triplicate unless other-wise stated. Statistical analyses were performed with the use of Origin software, version 8.6. Student's t-test was used to examine the statistical difference in FOXA2 and miR-199 expression between control and PDAC tissues. The

correlation significance was determined by means of Spearman and Pearson correlation analyses. A P-value of < 0.05 was considered statistically significant (*P < 0.05, **P< 0.01, ***P<0.001).

Ingenuity Network Software (IPA)

Gene network was constructed and important hubs were identified using Ingenuity Pathway Analysis (IPA; Ingenuity Systems, Mountain View, CA) based on the differentially expressed genes identified after inhibition of FOXA2 expression by siRNA FOXA2#2 in X pancreatic cancer cell line. IPA is a robust and expertly curated database containing updated information on more than 20,000 mammalian genes and proteins, 1.4 million biological interactions, and 100 canonical pathways incorporating over 6,000 discreet gene concepts. This information is integrated with relevant databases such as Entrez-Gene and Gene Ontology. The experimental data sets were used to query the IPA and to compose a set of interactive networks taking into consideration canonical pathways, the relevant biological interactions, and the cellular and disease processes. Pathways of highly interconnected genes were identified by statistical likelihood using the following equation:

$$Score = -\log_{10}\left(1 - \sum_{i=0}^{f-1} \frac{C(G,i)C(N-G,s-i)}{C(N,s)}\right)$$

Where N is the number of genes in the network of which G are central node genes, for a pathway of s genes of which f are central node genes. $C(n,k)$ is the binomial coefficient. We considered statistically significant networks those with a score greater than 5 (p value $<10^{-5}$).

RESULTS

FOXA2 transcription factor is down-regulated in human pancreatic cancers.

To evaluate the role of the human transcriptome in pancreatic oncogenesis, first we examined the expression levels of all the known transcription factors by performing gene profiling analysis in eight pancreatic control and fourteen PDAC tissues. This analysis revealed 43 transcription factors that were deregulated (>1.5 fold) in PDAC relative to control tissues (**Figure 1A, Table 1**). Interestingly, among the top differentially expressed transcription factors were FOXA2 (HNF-3β), HNF-1β and HNF-6, three members of the hepatocyte nuclear factor family of transcription factors (**Figure 1B**). Although the HNF family members are known to be involved in liver oncogenesis (25), their role in pancreatic oncogenesis has not been evaluated. The profiling analysis showed FOXA2 mRNA to be highly down-regulated in PDAC relative to control tissues, suggesting a potential tumor suppressor role in PDAC. To further validate the gene expression findings, we performed quantitative real-time PCR to examine FOXA2 mRNA expression levels in 14 control and 14 PDAC tissues in a second cohort of pancreatic cancer patients. Consistent with our initial findings, FOXA2 mRNA levels were significantly downregulated in PDAC (**Figure 1C**). In addition, we performed immunohistochemical (IHC) analysis for FOXA2 in 63 human tissue sections, including 42 PDAC, 21 control pancreatic tissues and found that 31/42 (74%) of PDAC tumors had no expression of FOXA2, while FOXA2 was expressed in all of the control tissues (**Figure 1D**), further suggesting a potential tumor suppressor role of FOXA2 in PDAC. In order to investigate the role of FOXA2 expression in pancreatic oncogenesis, we performed immunohistochemical analysis for FOXA2 in 3-month and 9-month old KC mice. Consistent with the human data, expression of FOXA2 was decreased in the 9-month old mice compared to the 3-month old mice **(Figure 1E),** suggesting that FOXA2 expression is decreased during pancreatic oncogenesis. Overall, all these data show that FOXA2 mRNA and protein levels are decreased in PDAC.

FOXA2 has tumor suppressor properties in PDAC.

To study the functional role of FOXA2 in pancreatic cancer, we screened a panel of seven (PANC-1, BxPC-3, HPAF-II, Capan-1, Capan-2, AsPC-1, MiaPaCa-2) different human pancreatic cancer cell lines for FOXA2 expression. Out of the seven cell lines investigated, PANC-1, BxPC-3 and HPAF-II expressed FOXA2 mRNA and were selected to perform further molecular studies by manipulating FOXA2 expression levels. We silenced FOXA2 expression by using two different siRNAs in two pancreatic cancer cell lines that exhibited increased FOXA2 levels (PANC-1 and BxPC-3). Cell growth analysis was studied and comparisons were performed relative to the cells transfected with an siRNA negative control (**Figure 2A**). Although siRNA#2 had a higher knockdown efficiency than siRNA#1 against FOXA2 (*data not shown*), when cells were transfected with either siRNA#1 or siRNA#2, a statistically significant increase in cell growth was observed in both PANC-1 and BxPC-3 cell lines, 48 hours post transfection (**Figure 2A**). Due to the higher knockdown efficiency, siRNA#2 was used in the follow-up experiments to manipulate FOXA2 levels *in vitro*. Specifically, FOXA2 inhibition by siRNA#2 significantly increased the ability of PANC-1 cells to form colonies in soft agar (**Figure 2B**). To further explore the functional role of FOXA2 in pancreatic cancer cell properties, we performed cell migration and invasion assays in PANC-1 (**Figure 2C and D**) and BxPC-3 cells (**Figure 2E and F**). A statistically significant higher number of migrating and invading cells were observed upon FOXA2 knockdown, suggesting that inhibition of FOXA2, promotes pancreatic oncogenesis. In order to explore the role of FOXA2 overexpression on invasion, FOXA2 was overexpressed in MiaPaCa-2 cells, a human pancreatic cancer cell line that does not express basal levels of FOXA2. There was a statistically significant difference in invasion upon FOXA2 overexpression, with a significant decrease in invasion upon FOXA2 overexpression compared to control **(Figure 2G)**.

MiR-199a negatively regulates FOXA2 expression through binding in its 3'UTR.

We were interested in identifying the molecular mechanism involved in the suppression of FOXA2 expression in pancreatic cancer. Initial DNA methylation analysis (Infinium HumanMethylation450 BeadChip assay) on 20 PDAC human tissues and 15 cancer adjacent normal tissues revealed that the FOXA2 promoter region was not differentially methylated in PDAC (*data not shown*), suggesting that DNA methylation is not the molecular mechanism responsible for FOXA2 reduced expression in pancreatic cancer. According to our previous studies, microRNAs have been found to be essential regulators of transcription factors involved in oncogenesis (34). Bioinformatics analysis by using the TargetScan algorithm revealed that miR-199a-3p has sequence complementarity in the position of 275-81 nt of the 3'UTR of FOXA2 (**Figure 3A**). To examine the direct interaction between miR-199a and FOXA2, we performed a 3'UTR luciferase assay. MiR-199 was overexpressed in Mia PaCa-2 cells that were co-transfected with a construct harboring the 3'UTR of FOXA2 under luciferase activity. We found that miR-199a overexpression reduced FOXA2 3'UTR luciferase activity compared to control and point mutation of the miR-199a binding site in the 3'UTR FOXA2 luciferase vector abolished the suppressive effects of miR-199a (**Figure 3B**). To further validate the interaction between miR-199a and FOXA2 *in vitro*, miR-199 was overexpressed in PANC-1 cells. We examined FOXA2 mRNA and protein levels, and found that FOXA2 levels significantly decreased in miR-199a-overexpressing pancreatic cancer cells (**Figure 3C, D**). Taken together, these findings suggest that miR-199a is a direct regulator of FOXA2 expression in pancreatic cancer.

MiR-199a has an oncogenic function in PDAC.

Next, we were interested in investigating the relevance of miR-199a in human pancreatic cancer. We performed real-time PCR analysis in 19 control and 17 PDAC tissues and found a statistically significant up-regulation of miR-199 expression in PDAC compared to control (**Figure 4A**). In order to examine the up-regulation of miR-199a in histological tissues, we

performed *in situ* hybridization on a tissue microarray containing 25 cases of pancreas adenocarcinoma with matched cancer adjacent tissue. *In situ* hybridization revealed 17/25 (68%) of adenocarcinomas highly expressed miR-199a (bottom panel), while it was not expressed in control tissues (upper panel) (**Figure 4B**). To explore the functional role of miR-199 in pancreatic oncogenesis we used the xCELLigence technology to monitor cell growth over a period of 120 hours, with a measurement taken every 15 minutes. This assay showed that miR-199a significantly increases the growth of PANC-1 cells (**Figure 4C**). Cell growth was also performed with the same experimental samples using the CellTiter-Glo Luminescent Cell Viability assay. MiR-199a overexpression led to a 50% increase in PANC-1 cell growth compared to cells transfected with a microRNA negative control (**Figure 4C**). To further assess the functional effects of miR-199a overexpression in pancreatic cancer, we performed migration and invasion assays in PANC-1 cells and found a statistically higher number of migrating and invading cells in the miR-199a-overexpressing PANC-1 cells relative to cells transfected with the microRNA negative control (**Figure 4D and E**).

FOXA2-regulated gene network in PDAC.

Our data revealed that FOXA2 has tumor suppressor properties in PDAC and its expression is regulated by miR-199a. To evaluate the molecular mechanisms that are regulated by FOXA2 suppression in PDAC and identify its downstream gene targets, we transiently knocked down FOXA2 using siFOXA2#2 in PANC-1 cells and its corresponding negative control, demonstrating an 80% inhibition of FOXA2 mRNA expression levels (**Figure 5A**). Next, we performed gene profiling analysis and found that 372 genes were up-regulated, while 552 were down-regulated (924 genes in total) in siFOXA2#2 PANC-1 cells relative to siRNA negative control by using a cut-off of $p<0.05$ and a fold change of 2 (**Figure 5B**). The Ingenuity Pathway Analysis (IPA) software was employed to perform signaling pathway analysis. The results revealed statistically significant enrichment for the cell movement/invasion pathway, cell proliferation, PI3K/AKT and MAPK signaling pathways (**Figure 5C**). To further evaluate these

481 findings we performed gene network analysis by using the 924 differentially expressed genes in
482 the IPA software network analysis and found that the most significant (p value $=10^{-42}$) gene
483 network was involved in cellular invasion having PLAUR, extracellular signal-regulated kinases
484 (ERK), and phosphoinositide 3-kinase (PI3K) as central nodes, consistent with our pathway
485 analysis (**Figure 5D**). Consistent with IPA network analysis data, inhibition of FOXA2 in
486 HPAF-II cells leads to activation of ERK, demonstrated by ERK phosphorylation (**Figure 5E**),
487 suggesting that FOXA2 suppression directly or indirectly leads to ERK activation. Interestingly,
488 PLAUR is a gene known to be related to cancer cell invasiveness and motility (14, 29, 67). To
489 further validate the gene network findings, we examined PLAUR expression levels by real-time
490 PCR after FOXA2 inhibition by siRNA#2. Consistent with our initial findings, FOXA2
491 inhibition resulted in a significant increase in PLAUR mRNA levels in PANC-1 cells (**Figure**
492 **5F**). To examine if PLAUR is mediating FOXA2 effects on pancreatic cancer cell invasiveness,
493 we performed an invasion assay knocking down either FOXA2 or both FOXA2 and PLAUR by
494 siRNAs in HPAF-II cells, a pancreatic cell line that expresses basal levels of both FOXA2 and
495 PLAUR. We observed a significant increase in invasion by knockdown of FOXA2 and this
496 increase in invasion was completely reversed when cells were transfected with both an siRNA
497 against FOXA2 and an siRNA against PLAUR (**Figure 5G**), suggesting that PLAUR is a major
498 mediator of FOXA2 effects on pancreatic cell invasiveness. Taken together, these data suggest
499 that FOXA2 regulates pancreatic cell invasiveness through regulation of PLAUR expression
500 levels.
501 Furthermore, it is known that microRNAs have multiple downstream gene targets and recent
502 studies have shown that the NF-kB pathway, which is affected by miR-199a, cross-talks with the
503 FOXA2 signaling pathway (49). To shed some light on the potential cross talk between FOXA2
504 and other common oncogenic pathways like nuclear factor-κB (NF-κB), we looked at the
505 expression of IL6, a downstream target of NF-kB, upon transient inhibition of FOXA2 in the
506 BxPC-3 cell line. Upon knockdown of FOXA2 with siRNA#2, there is a significant increase in
507 IL6 levels **(Figure 5H)**, indicating activation of the NF-kB pathway.

Generating a FOXA2Δ pancreatic cell line using the *CRISPR/Cas9 system.*

We observed the effects of FOXA2 inhibition of expression *in vitro* through a series of functional and gene expression assays. In order to study the effects of FOXA2 deletion *in vivo*, we developed a cell line with a permanent knock-out of FOXA2 at the chromosomal level (FOXA2Δ). We used the CRISPR/Cas9 system, where we co-transfected PANC-1 cells with two FOXA2 gRNA vectors, containing two different target sequences (**Figure 6A**) and the corresponding donor control vector. After clonal selection in puromycin, we validated FOXA2Δ at the protein level (**Figure 6B**) and also found a significant increase in PLAUR mRNA levels in FOXA2Δ compared to control (**Figure 6C**), consistent with our siRNA experimental setting. Next, we examined the phosphorylation levels of ERK and AKT by western blot and found both kinases to be activated in FOXA2Δ compared to control, consistent with our gene network analysis (**Figure 6D and E**). Conclusively, this data demonstrates the high efficiency of the CRISPR/Cas9 system, its consistency with the siRNA system, providing us with a powerful tool to study the role of FOXA2 *in vivo*.

CRISPR/Cas9 FOXA2 Inhibition suppresses pancreatic tumor growth in vivo.

To further support the role of FOXA2 as a tumor suppressor gene in pancreatic cancer, we wanted to test its properties *in vivo*. We performed subcutaneous injections in NOD/SCID mice with either FOXA2Δ PANC-1 ($5x10^5$ cells) or its corresponding PANC-1 control cell line (n=10/group). On day 64, mice were sacrificed and tumors were isolated. The FOXA2Δ tumor volumes (mm^3) and weight (g) were significantly larger than the PANC-1 control tumors (**Figure 7A, B and C**). On day 64, RNA was isolated from each tumor and quantitative real-time PCR showed that FOXA2 was not expressed in the FOXA2Δ tumors relative to controls (**Figure 7D**). Furthermore, in accordance with our *in vitro* findings, FOXA2Δ tumors showed increased PLAUR mRNA levels (**Figure 7E**). Moreover, E-cadherin levels decreased in FOXA2Δ tumors, indicating FOXA2 may also regulate cellular motility (**Figure 7F**). Taken

together, the *in vivo* data suggest that inhibition of FOXA2 increases the pancreatic tumorigenicity and aggressiveness.

DISCUSSION

Our study revealed FOXA2 as a novel tumor suppressor gene in pancreatic cancer. FOXA2 is a 455-amino acid member of the forkhead class of DNA-binding proteins and contains a highly conserved winged-helix DNA-binding domain (56). FOXA2 is a transcription factor that was initially identified in hepatocytes, where it binds in the promoter areas of important liver-enriched genes transthyretin, alpha 1-antitrypsin and albumin (13, 19, 28). It is required for the formation of the node, notochord, nervous system, and endoderm-derived structures (19, 36). In adulthood, FOXA2 has been shown to control metabolic homeostasis and to contribute to insulin resistance (65).

In the last decade, several studies have implicated the role of FOXA2 in solid tumors. FOXA2 has been found to be expressed in all types of neuroendocrine lung tumors (37) and shown to be a key regulator in colorectal liver metastases (43). We found that FOXA2 inhibition induces cancer cell invasiveness, consistent with its function in other cancers. Specifically, in human lung cancer cells, upon TGF-β1 treatment, FOXA2 levels are decreased, leading to activation of Slug transcription, thus inducing epithelial-mesenchymal transition (EMT) and promoting invasion (61). More recently, Liu et al. demonstrated FOXA2 phosphorylation by TNFα-induced IKKα stimulates the NOTCH1 pathway to promote liver cell proliferation and growth, indicating FOXA2 suppression by phosphorylation plays an important role in TNFα mediated tumorigenesis (49).

Although dysregulation of FOXA2 has been directly linked to the progression of certain cancers, this class of transcription factors can paradoxically serve as both tumor suppressors and

oncogenes (41). Very little is known about the roles of FOXA2 in invasion and tumor metastasis in pancreatic cancer. Our study identifies the transcription factors differentially expressed in PDAC and shows that FOXA2, and other hepatocyte nuclear factors, are significantly downregulated in human PDAC. Knockdown of FOXA2 led to a significant increase in cellular growth, migration, invasion and colony formation, indicating that FOXA2 harbors tumor suppressive properties.

Recent advances in pancreatic cancer biology have emerged important roles for microRNAs (miRNAs) in regulating tumor responses. MiRNAs, a class of non-coding RNAs, have emerged as critical players in cancer initiation and progression by modulating many pathological aspects related to tumor development, growth, metastasis, and drug resistance (48). Studies have found that miRNAs control many cellular processes through involvement in development, proliferation, the stress response, apoptosis, cell cycle progression, and differentiation (3, 5, 6, 16, 47). The major function of miRNAs is to post-transcriptionally regulate gene expression depending on recognition of complementary sequence residing in target mRNAs. Several key oncogenic miRNAs have been identified in pancreatic cancer, including miR-483-3p, miR-155, miR-21/miR-221, miR-27a, miR-371-5p and miR-21/miR-23a/miR-27a. Inhibition of oncogenic miRNAs reduces functional properties of pancreatic oncogenesis (18, 23, 24, 26, 52, 57). Our data indicate that miR-199a-3p plays an oncogenic role, with a significant increase in expression in PDAC compared to control. In the last decade, investigations have revealed that the expression of miRNA-199 is altered in several human cancers (22, 42, 70). Specifically, the expression of miRNA-199 is increased in ovarian cancer cells and cervical carcinomas (22, 70) in accordance to our data in PDAC. Specifically, overexpression of miR-199 in pancreatic cancer cells led to an increase in pancreatic cell growth, migration and invasion *in vitro*, demonstrating miR-199 oncogenic properties in pancreatic cancer.

We found that miR-199a-3p directly regulates FOXA2 mRNA and protein expression, through binding in its 3'UTR. Furthermore, recent studies have identified additional downstream targets of miR-199 in other cancer types. For example, miR-199 targets Frizzled type 7 receptor (FZD7), one of the most important Wnt receptors involved in cancer development and progression (59). Additionally, mTOR, c-MET, IKKβ, MET proto-oncogene and CD44 have also been identified as direct targets of miR-199, playing a major role in cancer initiation and progression in different types of cancer (10, 17, 21, 27, 39).

Conventionally, loss of function genetic screens in cultured cells is mainly conducted with the aid of RNA interference (RNAi) libraries (8, 71). However, RNAi could only partially and temporary suppress gene expression and thus its application is limited to knockdown screens (8, 54). Moreover, due to the endogenous nature of the RNAi pathway, it often incurs pervasive off-target events because of the extensive endogenous interactions. These off-target effects may confound the interpretation of screen results (35). Recently, the emergence of CRISPR/Cas9 technique offers a novel and versatile platform for genetic screen studies (4, 11, 53). For these reasons, we chose the highly efficient CRISPR/Cas9 deletion system to permanently knock-out FOXA2 in a pancreatic cancer cell line to study its effects *in vivo*. In addition, inhibition of FOXA2 expression levels by CRISPR/Cas9 *in vitro*, led to the activation of PLAUR gene, which is known to be involved in cancer invasiveness (38). Importantly, these findings were consistent with our data where FOXA2 expression was suppressed by siRNA, suggesting that the CRISPR/Cas9 system is very effective to block gene expression in cancer cells. Taken together, our study has revealed a novel signaling pathway, consisting of the miR-199 and FOXA2 tumor suppressor gene involved in pancreatic oncogenesis.

GRANTS

This study was supported by start-up funds to D.I. and by the Pancreatic Cancer Network-AACR (PanCan-AACR) grant to D.I.

DISCLOSURE

No conflicts of interest, financial or otherwise, are declared by the author(s).

AUTHOR CONTRIBUTIONS

C.V., M.H. and DI developed the concept and designed the research; C.V., M.K. G.E. and J.W., performed the experiments; C.V., M.H., S.M. analyzed the data and interpreted the results of the experiment; C.V. prepared the figures and drafted the manuscript; J.W, T.R.D. and G.A.P. provided human pancreatic tissues for experiments; All the authors edited, revised and approved the final version of the manuscript.

REFERENCES

1. Aguirre AJ, Bardeesy N, Sinha M, Lopez L, Tuveson DA, Horner J, Redston MS, and DePinho RA. Activated Kras and Ink4a/Arf deficiency cooperate to produce metastatic pancreatic ductal adenocarcinoma. *Genes Dev* **17**: 3112-3126, 2003.
2. Almoguera C, Shibata D, Forrester K, Martin J, Arnheim N, and Perucho M. Most human carcinomas of the exocrine pancreas contain mutant c-K-ras genes. *Cell* **53**: 549-554, 1988.
3. Ambros V. The functions of animal microRNAs. *Nature* **431**: 350-355, 2004.
4. Barrangou R, Fremaux C, Deveau H, Richards M, Boyaval P, Moineau S, Romero DA, and Horvath P. CRISPR provides acquired resistance against viruses in prokaryotes. *Science* **315**: 1709-1712, 2007.
5. Bartel DP. MicroRNAs: genomics, biogenesis, mechanism, and function. *Cell* **116**: 281-297, 2004.
6. Bartel DP. MicroRNAs: target recognition and regulatory functions. *Cell* **136**: 215-233, 2009.
7. Bondar VM, Sweeney-Gotsch B, Andreeff M, Mills GB, and McConkey DJ. Inhibition of the phosphatidylinositol 3'-kinase-AKT pathway induces apoptosis in pancreatic carcinoma cells in vitro and in vivo. *Mol Cancer Ther* **1**: 989-997, 2002.
8. Boutros M and Ahringer J. The art and design of genetic screens: RNA interference. *Nat Rev Genet* **9**: 554-566, 2008.
9. Burris HA, 3rd, Moore MJ, Andersen J, Green MR, Rothenberg ML, Modiano MR, Cripps MC, Portenoy RK, Storniolo AM, Tarassoff P, Nelson R, Dorr FA, Stephens CD, and Von Hoff DD.

648 Improvements in survival and clinical benefit with gemcitabine as first-line therapy for patients with
649 advanced pancreas cancer: a randomized trial. *J Clin Oncol* **15**: 2403-2413, 1997.
650 10. Cheng W, Liu T, Wan X, Gao Y, and Wang H. MicroRNA-199a targets CD44 to suppress the
651 tumorigenicity and multidrug resistance of ovarian cancer-initiating cells. *FEBS J* **279**: 2047-2059, 2012.
652 11. Cong L, Ran FA, Cox D, Lin S, Barretto R, Habib N, Hsu PD, Wu X, Jiang W, Marraffini LA, and
653 Zhang F. Multiplex genome engineering using CRISPR/Cas systems. *Science* **339**: 819-823, 2013.
654 12. Corcoran RB, Contino G, Deshpande V, Tzatsos A, Conrad C, Benes CH, Levy DE, Settleman J,
655 Engelman JA, and Bardeesy N. STAT3 plays a critical role in KRAS-induced pancreatic tumorigenesis.
656 *Cancer Res* **71**: 5020-5029, 2011.
657 13. Costa RH, Grayson DR, and Darnell JE, Jr. Multiple hepatocyte-enriched nuclear factors function
658 in the regulation of transthyretin and alpha 1-antitrypsin genes. *Mol Cell Biol* **9**: 1415-1425, 1989.
659 14. Cozzi PJ, Wang J, Delprado W, Madigan MC, Fairy S, Russell PJ, and Li Y. Evaluation of urokinase
660 plasminogen activator and its receptor in different grades of human prostate cancer. *Hum Pathol* **37**:
661 1442-1451, 2006.
662 15. Dawson DW, Hertzer K, Moro A, Donald G, Chang HH, Go VL, Pandol SJ, Lugea A, Gukovskaya AS,
663 Li G, Hines OJ, Rozengurt E, and Eibl G. High-fat, high-calorie diet promotes early pancreatic neoplasia in
664 the conditional KrasG12D mouse model. *Cancer Prev Res (Phila)* **6**: 1064-1073, 2013.
665 16. Engels BM and Hutvagner G. Principles and effects of microRNA-mediated post-transcriptional
666 gene regulation. *Oncogene* **25**: 6163-6169, 2006.
667 17. Fornari F, Milazzo M, Chieco P, Negrini M, Calin GA, Grazi GL, Pollutri D, Croce CM, Bolondi L,
668 and Gramantieri L. MiR-199a-3p regulates mTOR and c-Met to influence the doxorubicin sensitivity of
669 human hepatocarcinoma cells. *Cancer Res* **70**: 5184-5193, 2010.
670 18. Frampton AE, Castellano L, Colombo T, Giovannetti E, Krell J, Jacob J, Pellegrino L, Roca-Alonso L,
671 Funel N, Gall TM, De Giorgio A, Pinho FG, Fulci V, Britton DJ, Ahmad R, Habib NA, Coombes RC, Harding
672 V, Knosel T, Stebbing J, and Jiao LR. MicroRNAs cooperatively inhibit a network of tumor suppressor
673 genes to promote pancreatic tumor growth and progression. *Gastroenterology* **146**: 268-277 e218,
674 2014.
675 19. Friedman JR and Kaestner KH. The Foxa family of transcription factors in development and
676 metabolism. *Cell Mol Life Sci* **63**: 2317-2328, 2006.
677 20. Fujioka S, Sclabas GM, Schmidt C, Frederick WA, Dong QG, Abbruzzese JL, Evans DB, Baker C,
678 and Chiao PJ. Function of nuclear factor kappaB in pancreatic cancer metastasis. *Clin Cancer Res* **9**: 346-
679 354, 2003.
680 21. Gao Y, Feng Y, Shen JK, Lin M, Choy E, Cote GM, Harmon DC, Mankin HJ, Hornicek FJ, and Duan
681 Z. CD44 is a direct target of miR-199a-3p and contributes to aggressive progression in osteosarcoma. *Sci*
682 *Rep* **5**: 11365, 2015.
683 22. Garzon R, Calin GA, and Croce CM. MicroRNAs in Cancer. *Annu Rev Med* **60**: 167-179, 2009.
684 23. Gironella M, Seux M, Xie MJ, Cano C, Tomasini R, Gommeaux J, Garcia S, Nowak J, Yeung ML,
685 Jeang KT, Chaix A, Fazli L, Motoo Y, Wang Q, Rocchi P, Russo A, Gleave M, Dagorn JC, Iovanna JL, Carrier
686 A, Pebusque MJ, and Dusetti NJ. Tumor protein 53-induced nuclear protein 1 expression is repressed by
687 miR-155, and its restoration inhibits pancreatic tumor development. *Proc Natl Acad Sci U S A* **104**:
688 16170-16175, 2007.
689 24. Hao J, Zhang S, Zhou Y, Hu X, and Shao C. MicroRNA 483-3p suppresses the expression of
690 DPC4/Smad4 in pancreatic cancer. *FEBS Lett* **585**: 207-213, 2011.
691 25. Hatziapostolou M, Polytarchou C, Aggelidou E, Drakaki A, Poultsides GA, Jaeger SA, Ogata H,
692 Karin M, Struhl K, Hadzopoulou-Cladaras M, and Iliopoulos D. An HNF4alpha-miRNA inflammatory
693 feedback circuit regulates hepatocellular oncogenesis. *Cell* **147**: 1233-1247, 2011.
694 26. He D, Miao H, Xu Y, Xiong L, Wang Y, Xiang H, Zhang H, and Zhang Z. MiR-371-5p facilitates
695 pancreatic cancer cell proliferation and decreases patient survival. *PLoS One* **9**: e112930, 2014.

696 27. Henry JC, Park JK, Jiang J, Kim JH, Nagorney DM, Roberts LR, Banerjee S, and Schmittgen TD.
697 miR-199a-3p targets CD44 and reduces proliferation of CD44 positive hepatocellular carcinoma cell
698 lines. *Biochem Biophys Res Commun* **403**: 120-125, 2010.
699 28. Herbst RS, Nielsch U, Sladek F, Lai E, Babiss LE, and Darnell JE, Jr. Differential regulation of
700 hepatocyte-enriched transcription factors explains changes in albumin and transthyretin gene
701 expression among hepatoma cells. *New Biol* **3**: 289-296, 1991.
702 29. Hildenbrand R and Schaaf A. The urokinase-system in tumor tissue stroma of the breast and
703 breast cancer cell invasion. *Int J Oncol* **34**: 15-23, 2009.
704 30. Hingorani SR, Petricoin EF, Maitra A, Rajapakse V, King C, Jacobetz MA, Ross S, Conrads TP,
705 Veenstra TD, Hitt BA, Kawaguchi Y, Johann D, Liotta LA, Crawford HC, Putt ME, Jacks T, Wright CV,
706 Hruban RH, Lowy AM, and Tuveson DA. Preinvasive and invasive ductal pancreatic cancer and its early
707 detection in the mouse. *Cancer Cell* **4**: 437-450, 2003.
708 31. Hingorani SR, Wang L, Multani AS, Combs C, Deramaudt TB, Hruban RH, Rustgi AK, Chang S, and
709 Tuveson DA. Trp53R172H and KrasG12D cooperate to promote chromosomal instability and widely
710 metastatic pancreatic ductal adenocarcinoma in mice. *Cancer Cell* **7**: 469-483, 2005.
711 32. Hruban RH, Adsay NV, Albores-Saavedra J, Compton C, Garrett ES, Goodman SN, Kern SE,
712 Klimstra DS, Kloppel G, Longnecker DS, Luttges J, and Offerhaus GJ. Pancreatic intraepithelial neoplasia:
713 a new nomenclature and classification system for pancreatic duct lesions. *Am J Surg Pathol* **25**: 579-586,
714 2001.
715 33. Hruban RH, van Mansfeld AD, Offerhaus GJ, van Weering DH, Allison DC, Goodman SN, Kensler
716 TW, Bose KK, Cameron JL, and Bos JL. K-ras oncogene activation in adenocarcinoma of the human
717 pancreas. A study of 82 carcinomas using a combination of mutant-enriched polymerase chain reaction
718 analysis and allele-specific oligonucleotide hybridization. *Am J Pathol* **143**: 545-554, 1993.
719 34. Iliopoulos D, Jaeger SA, Hirsch HA, Bulyk ML, and Struhl K. STAT3 activation of miR-21 and miR-
720 181b-1 via PTEN and CYLD are part of the epigenetic switch linking inflammation to cancer. *Mol Cell* **39**:
721 493-506, 2010.
722 35. Jackson AL, Bartz SR, Schelter J, Kobayashi SV, Burchard J, Mao M, Li B, Cavet G, and Linsley PS.
723 Expression profiling reveals off-target gene regulation by RNAi. *Nat Biotechnol* **21**: 635-637, 2003.
724 36. Kaestner KH, Lee KH, Schlondorff J, Hiemisch H, Monaghan AP, and Schutz G. Six members of the
725 mouse forkhead gene family are developmentally regulated. *Proc Natl Acad Sci U S A* **90**: 7628-7631,
726 1993.
727 37. Khoor A, Stahlman MT, Johnson JM, Olson SJ, and Whitsett JA. Forkhead box A2 transcription
728 factor is expressed in all types of neuroendocrine lung tumors. *Hum Pathol* **35**: 560-564, 2004.
729 38. Kim J, Yu W, Kovalski K, and Ossowski L. Requirement for specific proteases in cancer cell
730 intravasation as revealed by a novel semiquantitative PCR-based assay. *Cell* **94**: 353-362, 1998.
731 39. Kim S, Lee UJ, Kim MN, Lee EJ, Kim JY, Lee MY, Choung S, Kim YJ, and Choi YC. MicroRNA miR-
732 199a* regulates the MET proto-oncogene and the downstream extracellular signal-regulated kinase 2
733 (ERK2). *J Biol Chem* **283**: 18158-18166, 2008.
734 40. Klein WM, Hruban RH, Klein-Szanto AJ, and Wilentz RE. Direct correlation between proliferative
735 activity and dysplasia in pancreatic intraepithelial neoplasia (PanIN): additional evidence for a recently
736 proposed model of progression. *Mod Pathol* **15**: 441-447, 2002.
737 41. Lee CS, Friedman JR, Fulmer JT, and Kaestner KH. The initiation of liver development is
738 dependent on Foxa transcription factors. *Nature* **435**: 944-947, 2005.
739 42. Lee JW, Choi CH, Choi JJ, Park YA, Kim SJ, Hwang SY, Kim WY, Kim TJ, Lee JH, Kim BG, and Bae DS.
740 Altered MicroRNA expression in cervical carcinomas. *Clin Cancer Res* **14**: 2535-2542, 2008.
741 43. Lehner F, Kulik U, Klempnauer J, and Borlak J. The hepatocyte nuclear factor 6 (HNF6) and
742 FOXA2 are key regulators in colorectal liver metastases. *FASEB J* **21**: 1445-1462, 2007.
743 44. Li D, Xie K, Wolff R, and Abbruzzese JL. Pancreatic cancer. *Lancet* **363**: 1049-1057, 2004.

744 45. Li J, Zhang Y, Gao Y, Cui Y, Liu H, Li M, and Tian Y. Downregulation of HNF1 homeobox B is
745 associated with drug resistance in ovarian cancer. *Oncol Rep* **32**: 979-988, 2014.
746 46. Li J and Zhou BP. Activation of beta-catenin and Akt pathways by Twist are critical for the
747 maintenance of EMT associated cancer stem cell-like characters. *BMC Cancer* **11**: 49, 2011.
748 47. Lim LP, Lau NC, Garrett-Engele P, Grimson A, Schelter JM, Castle J, Bartel DP, Linsley PS, and
749 Johnson JM. Microarray analysis shows that some microRNAs downregulate large numbers of target
750 mRNAs. *Nature* **433**: 769-773, 2005.
751 48. Ling H, Fabbri M, and Calin GA. MicroRNAs and other non-coding RNAs as targets for anticancer
752 drug development. *Nat Rev Drug Discov* **12**: 847-865, 2013.
753 49. Liu M, Lee DF, Chen CT, Yen CJ, Li LY, Lee HJ, Chang CJ, Chang WC, Hsu JM, Kuo HP, Xia W, Wei Y,
754 Chiu PC, Chou CK, Du Y, Dhar D, Karin M, Chen CH, and Hung MC. IKKalpha activation of NOTCH links
755 tumorigenesis via FOXA2 suppression. *Mol Cell* **45**: 171-184, 2012.
756 50. Liu YN, Lee WW, Wang CY, Chao TH, Chen Y, and Chen JH. Regulatory mechanisms controlling
757 human E-cadherin gene expression. *Oncogene* **24**: 8277-8290, 2005.
758 51. Luttges J, Galehdari H, Brocker V, Schwarte-Waldhoff I, Henne-Bruns D, Kloppel G, Schmiegel W,
759 and Hahn SA. Allelic loss is often the first hit in the biallelic inactivation of the p53 and DPC4 genes
760 during pancreatic carcinogenesis. *Am J Pathol* **158**: 1677-1683, 2001.
761 52. Ma Y, Yu S, Zhao W, Lu Z, and Chen J. miR-27a regulates the growth, colony formation and
762 migration of pancreatic cancer cells by targeting Sprouty2. *Cancer Lett* **298**: 150-158, 2010.
763 53. Mali P, Yang L, Esvelt KM, Aach J, Guell M, DiCarlo JE, Norville JE, and Church GM. RNA-guided
764 human genome engineering via Cas9. *Science* **339**: 823-826, 2013.
765 54. Mohr SE, Smith JA, Shamu CE, Neumuller RA, and Perrimon N. RNAi screening comes of age:
766 improved techniques and complementary approaches. *Nat Rev Mol Cell Biol* **15**: 591-600, 2014.
767 55. Moskaluk CA, Hruban RH, and Kern SE. p16 and K-ras gene mutations in the intraductal
768 precursors of human pancreatic adenocarcinoma. *Cancer Res* **57**: 2140-2143, 1997.
769 56. Pani L, Overdier DG, Porcella A, Qian X, Lai E, and Costa RH. Hepatocyte nuclear factor 3 beta
770 contains two transcriptional activation domains, one of which is novel and conserved with the
771 Drosophila fork head protein. *Mol Cell Biol* **12**: 3723-3732, 1992.
772 57. Park JK, Lee EJ, Esau C, and Schmittgen TD. Antisense inhibition of microRNA-21 or -221 arrests
773 cell cycle, induces apoptosis, and sensitizes the effects of gemcitabine in pancreatic adenocarcinoma.
774 *Pancreas* **38**: e190-199, 2009.
775 58. Rozenblum E, Schutte M, Goggins M, Hahn SA, Panzer S, Zahurak M, Goodman SN, Sohn TA,
776 Hruban RH, Yeo CJ, and Kern SE. Tumor-suppressive pathways in pancreatic carcinoma. *Cancer Res* **57**:
777 1731-1734, 1997.
778 59. Song J, Gao L, Yang G, Tang S, Xie H, Wang Y, Wang J, Zhang Y, Jin J, Gou Y, Yang Z, Chen Z, Wu K,
779 Liu J, and Fan D. MiR-199a regulates cell proliferation and survival by targeting FZD7. *PLoS One* **9**:
780 e110074, 2014.
781 60. Sureban SM, May R, Qu D, Weygant N, Chandrakesan P, Ali N, Lightfoot SA, Pantazis P, Rao CV,
782 Postier RG, and Houchen CW. DCLK1 regulates pluripotency and angiogenic factors via microRNA-
783 dependent mechanisms in pancreatic cancer. *PLoS One* **8**: e73940, 2013.
784 61. Tang Y, Shu G, Yuan X, Jing N, and Song J. FOXA2 functions as a suppressor of tumor metastasis
785 by inhibition of epithelial-to-mesenchymal transition in human lung cancers. *Cell Res* **21**: 316-326, 2011.
786 62. Thota R, Pauff JM, and Berlin JD. Treatment of metastatic pancreatic adenocarcinoma: a review.
787 *Oncology (Williston Park)* **28**: 70-74, 2014.
788 63. Wang Z, Li Y, Ahmad A, Banerjee S, Azmi AS, Kong D, and Sarkar FH. Pancreatic cancer:
789 understanding and overcoming chemoresistance. *Nat Rev Gastroenterol Hepatol* **8**: 27-33, 2011.

790 64. Wilentz RE, Iacobuzio-Donahue CA, Argani P, McCarthy DM, Parsons JL, Yeo CJ, Kern SE, and
791 Hruban RH. Loss of expression of Dpc4 in pancreatic intraepithelial neoplasia: evidence that DPC4
792 inactivation occurs late in neoplastic progression. *Cancer Res* **60**: 2002-2006, 2000.
793 65. Wolfrum C and Stoffel M. Coactivation of Foxa2 through Pgc-1beta promotes liver fatty acid
794 oxidation and triglyceride/VLDL secretion. *Cell Metab* **3**: 99-110, 2006.
795 66. Xia JT, Wang H, Liang LJ, Peng BG, Wu ZF, Chen LZ, Xue L, Li Z, and Li W. Overexpression of
796 FOXM1 is associated with poor prognosis and clinicopathologic stage of pancreatic ductal
797 adenocarcinoma. *Pancreas* **41**: 629-635, 2012.
798 67. Yamamoto M, Sawaya R, Mohanam S, Rao VH, Bruner JM, Nicolson GL, and Rao JS. Expression
799 and localization of urokinase-type plasminogen activator receptor in human gliomas. *Cancer Res* **54**:
800 5016-5020, 1994.
801 68. Yamano M, Fujii H, Takagaki T, Kadowaki N, Watanabe H, and Shirai T. Genetic progression and
802 divergence in pancreatic carcinoma. *Am J Pathol* **156**: 2123-2133, 2000.
803 69. Yan H, Wu J, Liu W, Zuo Y, Chen S, Zhang S, Zeng M, and Huang W. MicroRNA-20a
804 overexpression inhibited proliferation and metastasis of pancreatic carcinoma cells. *Hum Gene Ther* **21**:
805 1723-1734, 2010.
806 70. Yanaihara N, Caplen N, Bowman E, Seike M, Kumamoto K, Yi M, Stephens RM, Okamoto A,
807 Yokota J, Tanaka T, Calin GA, Liu CG, Croce CM, and Harris CC. Unique microRNA molecular profiles in
808 lung cancer diagnosis and prognosis. *Cancer Cell* **9**: 189-198, 2006.
809 71. Yang X, Boehm JS, Yang X, Salehi-Ashtiani K, Hao T, Shen Y, Lubonja R, Thomas SR, Alkan O,
810 Bhimdi T, Green TM, Johannessen CM, Silver SJ, Nguyen C, Murray RR, Hieronymus H, Balcha D, Fan C,
811 Lin C, Ghamsari L, Vidal M, Hahn WC, Hill DE, and Root DE. A public genome-scale lentiviral expression
812 library of human ORFs. *Nat Methods* **8**: 659-661, 2011.
813 72. Yauch RL and Settleman J. Recent advances in pathway-targeted cancer drug therapies emerging
814 from cancer genome analysis. *Curr Opin Genet Dev* **22**: 45-49, 2012.
815 73. Yuan XW, Wang DM, Hu Y, Tang YN, Shi WW, Guo XJ, and Song JG. Hepatocyte nuclear factor 6
816 suppresses the migration and invasive growth of lung cancer cells through p53 and the inhibition of
817 epithelial-mesenchymal transition. *J Biol Chem* **288**: 31206-31216, 2013.

818

819

820 **FIGURE LEGENDS**

821 **Figure 1.**

822 **FOXA2 transcription factor is down-regulated in human pancreatic cancers**. *A.* Pancreatic
823 cancer transcription factor transcriptome. Heatmap showing unsupervised clustering of
824 expression Z-scores of mRNA expression of 105 probes from 43 transcription factor genes in 22
825 human pancreatic tissue (control =7 and cancer =15). *B.* Expression levels of hepatocyte nuclear
826 factor family transcription factors (FOXA2, HNF-1β and HNF-6) from the list of 43
827 transcription factors differentially expressed in PDAC. *C.* FOXA2 mRNA levels by real-time
828 PCR in 28 human pancreatic tissue (control =14 and cancer =14). *D.* Immunohistochemical
829 staining for human FOXA2 in control (top panel) and PDAC tissue (bottom panel). *E.*
830 Immunohistochemical staining for mouse FOXA2 in 3-month old (top panel) and 9-month old

KrasG12D$^{+/-}$p48-Cre$^{+/-}$ (KC) mice (bottom panel). The experiments have been performed in triplicate and all data are represented as mean ± SD. ***P<0.001, **P<0.01, *P<0.05.

Figure 2.

FOXA2 has tumor suppressor gene properties in PDAC. *A.* Relative percent cell growth measured in PANC-1 and BxPC-3 treated for 48 h with siRNA negative control (siRNA NC) or two different siRNAs against FOXA2 (siFOXA2#1 and siFOXA2#2) using the Cell-Titer Glo Luminescence Cell Viability Assay. *B.* Soft agar colony formation assay of PANC-1 cells treated for 48 h with siRNA NC or siFOXA2#2. Colonies (mean ± SD) 50 mm were counted using a microscope 20 days later. *C.* Transwell cell migration assay in PANC-1 cells transfected with siRNA NC or siFOXA2#2, migrating across 8 mm micropore membranes. *D.* Invasion through matrigel-coated transwell inserts in PANC-1 cells transfected with siRNA NC or siFOXA2#2. *E.* Transwell cell migration assay in BxPC-3 cells transfected with siRNA NC or siFOXA2#2, migrating across 8 mm micropore membranes. *F.* Invasion through matrigel-coated transwell inserts in BxPC-3 cells transfected with siRNA NC or siFOXA2#2. *G.* Invasion through matrigel-coated transwell inserts in MiaPaCa-2 cells transfected with control vector (control) or FOXA2 overexpression vector (FOXA2 OE). The experiments have been performed in triplicate and all data are represented as mean ± SD. ***P<0.001, **P<0.01, *P<0.05.

Figure 3.

FOXA2 as a direct target of miR-199a-3p in PDAC. *A.*Sequence complimentarity between miR-199a-3p seed sequence and the 3'UTR of FOXA2. *B*. FOXA2 3'UTR luciferase activity in MIA PaCa-2 cells transfected with miR-NC or miR-199, 48 h post transfection. MiR-199 sequence was wildtype (miR 199) or mutated (miR mutant). *C*. FOXA2 relative mRNA levels in PANC-1 cell line 24 h post transfection with miR-199 mimic. *D.* Western blot showing FOXA2 protein levels in PANC-1 cell line 72 h post transfection with miR-199 mimic. The experiments have been performed in triplicate and all data are represented as mean ± SD. ***P<0.001, **P<0.01, *P<0.05.

Figure 4.

MiR-199 has an oncogenic function in PDAC. *A*. MiR-199 mRNA levels in human pancreatic control (n=19) and cancer tissue (n=17). *B. In situ* hybridization miR-199 in human pancreatic control and cancer tissue under 10X and 20X magnification. *C*. Cell proliferation in Panc-1 cells 24 h post transfection with miR negative control (miR-NC) or miR-199 mimic (miR-199) using the xCELLigence system. PANC-1 cells were seeded at a density of $5x10^3$ cells/well in 96-well

866 E-plates and monitored for 120 h. *D.* Percentage cell growth measured in BxPC-3 cells treated
867 with miR-NC or miR-199 for 24 h then plated and measured 48 h later using the Cell-Titer Glo
868 Luminescence Cell Viability Assay. *E*. Transwell cell migration assay in PANC-1 cells
869 transfected with miR-NC or miR-199. *F*. Invasion through matrigel-coated transwell inserts in
870 PANC-1 cells transfected with miR-NC or miR-199. The experiments have been performed in
871 triplicate and all data are represented as mean ± SD. ***P<0.001, **P<0.01, *P<0.05.

872

873 **Figure 5.**

874 **FOXA2-regulated gene network in PDAC**. *A*. Relative FOXA2 mRNA levels in PANC-1 cells
875 transfected with siRNA NC or siFOXA2#2 for gene profiling studies, duplicate experimental
876 samples were performed. *B.* Heatmap indicating expression levels of 372 genes up-regulated and
877 552 genes down-regulated in siRNA NC compared to siFOXA2#2 samples in PANC-1 cell line.
878 *C*. Ingenuity Pathway Analysis (IPA) reveals statistically significant enrichment for the cell
879 movement/invasion pathway, cell proliferation, PI3K/AKT and MAPK signaling pathways. *D.*
880 Gene network analysis by using the 924 differentially expressed genes in the IPA software
881 network found the most significant (p value $=10^{-42}$) gene network was involved in cellular
882 invasion having as central nodes PLAUR, ERK, PI3K, consistent with our gene ontology
883 analysis. *E*. Western blot indicating phosphorylation of ERK, total ERK and CREB in PANC-1
884 cells treated with siRNA NC or siFOXA2#2. *F*. PLAUR mRNA levels in HPAF-II cells treated
885 with siRNA NC or siFOXA2#2. *G.* Invasion through matrigel-coated transwell inserts in HPAF-
886 II cells transfected with siRNA NC, siFOXA2#2 or both siFOXA2#2 and siPLAUR. *H.* Relative
887 mRNA levels of IL6, assessed by rt-PCR in BxPC-3 cells transfected with siRNA NC or
888 siFOXA2#2.The experiments have been performed in triplicate and all data are represented as
889 mean ± SD. ***P<0.001, **P<0.01, *P<0.05.

890

891 **Figure 6.**

892 **Generating a FOXA2Δ pancreatic cell line using the CRISPR/Cas9 system**. *A.* Sequences of
893 FOXA2 gRNA vectors. PANC-1 cells were transfected with either 1.) two gRNA vectors and
894 donor vector (donor vector not shown) referred to as FOXA2Δ or 2.) a scramble vector and a
895 donor vector (scramble vector and donor vector not shown) referred to as PANC-1 control. *B.*
896 Western blot for PANC-1 control and FOXA2Δ generated cell lines. *C.* PLAUR mRNA
897 expression levels in PANC-1 control and FOXA2Δ cell lines. *D*. Western blot indicating
898 phosphorylation of ERK and total ERK plus loading control in PANC-1 control and FOXA2Δ
899 cell lines. *E*. Western blot indicating phosphorylation of AKT at two phosphorylation sites
900 (Ser473 and Thr308) and total AKT plus loading control in PANC-1 control and FOXA2Δ cell

901 lines. The experiments have been performed in triplicate and all data are represented as mean ±
902 SD. ***P<0.001, **P<0.01, *P<0.05.

903

904 **Figure 7.**

905 **CRISPR/Cas9 FOXA2 Inhibition suppresses pancreatic tumor growth *in vivo*.** *A*. At day 64,
906 tumor volumes (mm^3) were measured in PANC-1 control and FOXA2Δ (n=10/group) tumors. *B*.
907 At day 64, tumors were excised and tumor weight (g) was measured in PANC-1 control and
908 FOXA2Δ tumors. *C*. At day 64, PANC-1 control and FOXA2 tumors were excised and
909 photographed, pictured with ruler (mm). *D*. At day 64, RNA was isolated from tumors and
910 FOXA2 mRNA levels were examined in PANC-1 control and FOXA2Δ tumors. *E*. PLAUR
911 mRNA levels were examined in PANC-1 control and FOXA2Δ tumors. *F*. Relative E-cadherin
912 mRNA levels in PANC-1 control and FOXA2Δ tumors (n=10/group). The experiments have
913 been performed in triplicate and all data are represented as mean ± SD. ***P<0.001, **P<0.01,
914 *P<0.05.

Figure 1

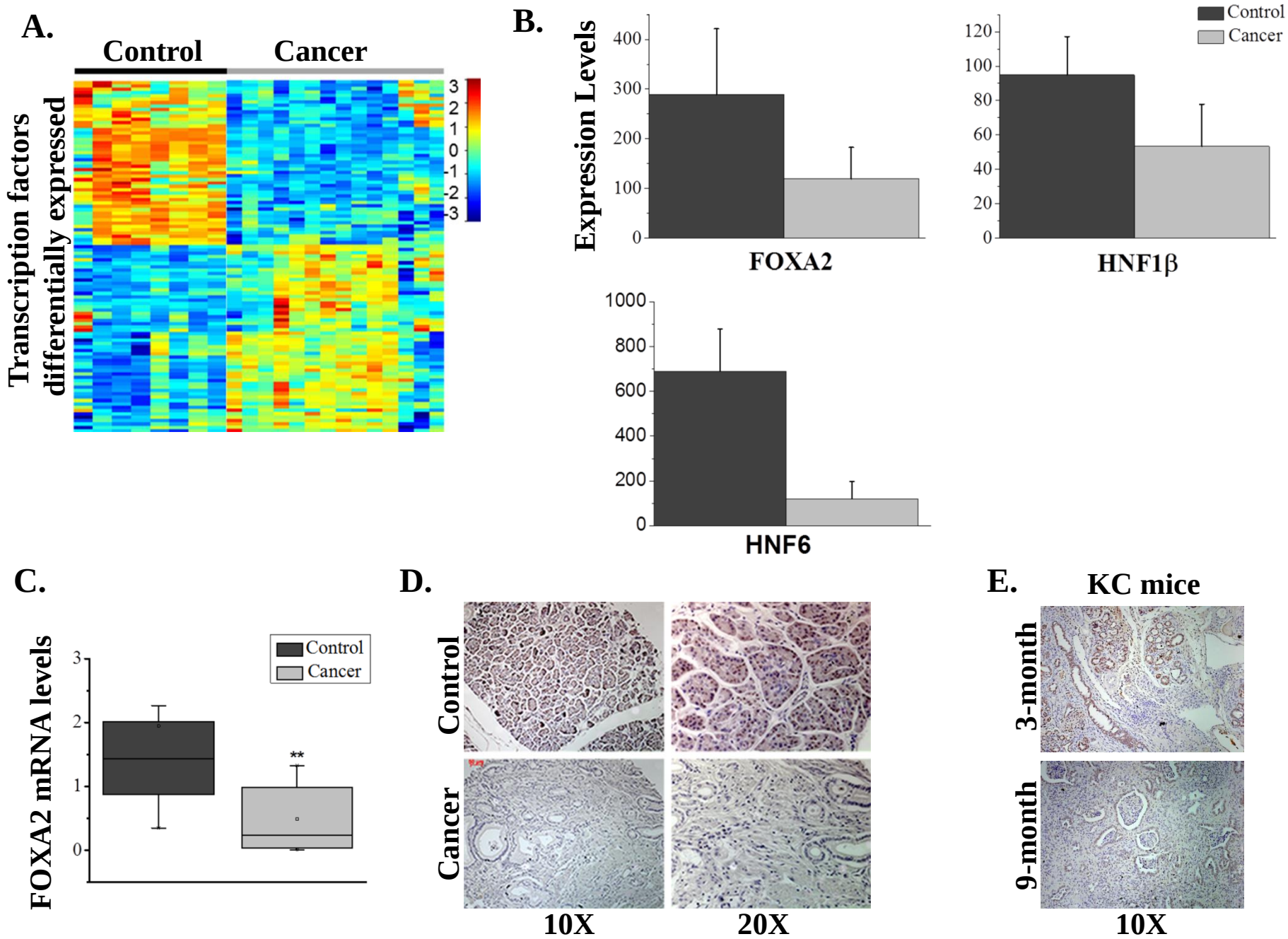
A.
Control
Cancer
Transcription factors differentially expressed
3
2
1
0
-1
-2
-3
B.
Expression Levels
Control
Cancer
FOXA2
HNF1β
HNF6
C.
FOXA2 mRNA levels
Control
Cancer
**
D.
Control
Cancer
10X
20X
E.
KC mice
3-month
9-month
10X

Figure 2

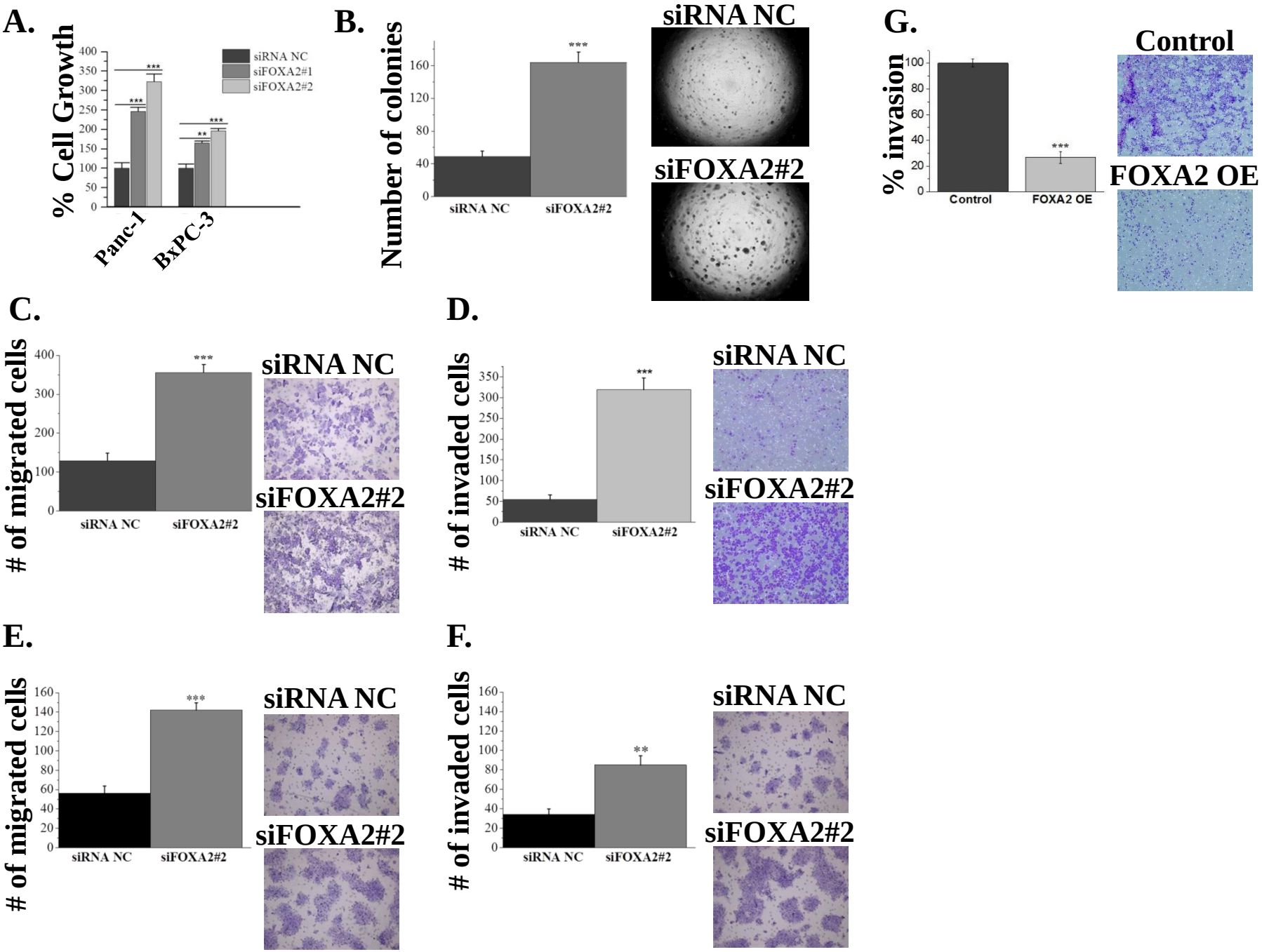
A.
% Cell Growth
siRNA NC
siFOXA2#1
siFOXA2#2
Panc-1
BxPC-3
B.
Number of colonies
siRNA NC
siFOXA2#2
C.
# of migrated cells
D.
# of invaded cells
E.
# of migrated cells
F.
# of invaded cells
G.
% invasion
Control
FOXA2 OE

Figure 3

A.

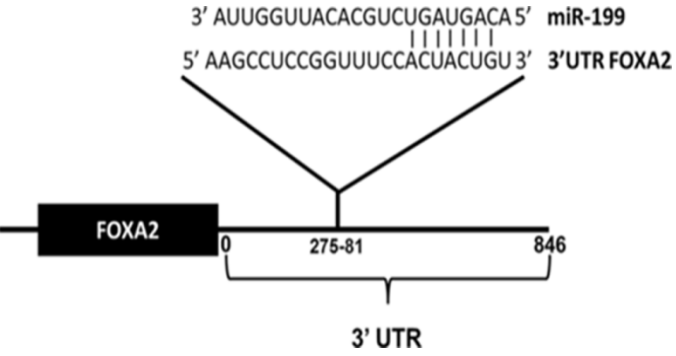

B.

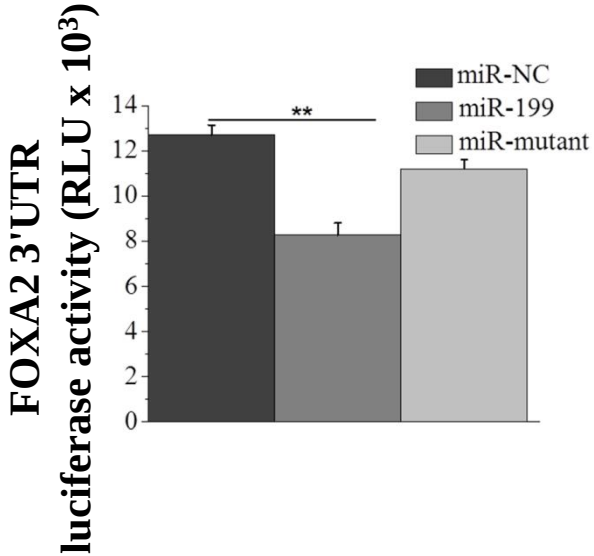

C.

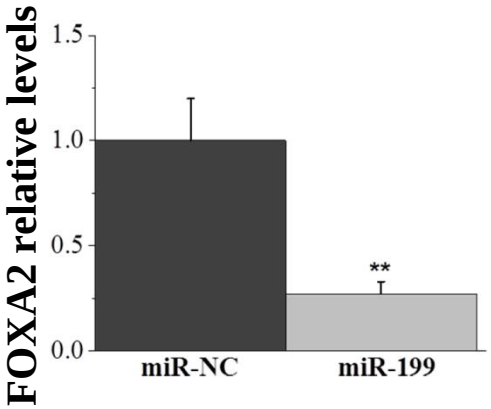

D.

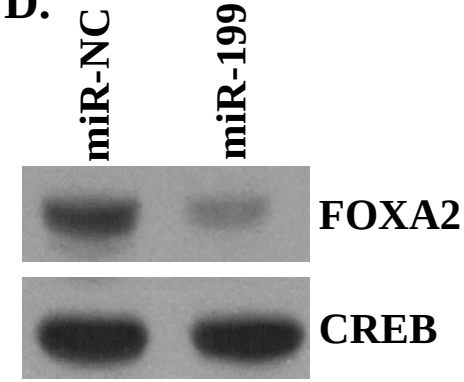

Figure 4

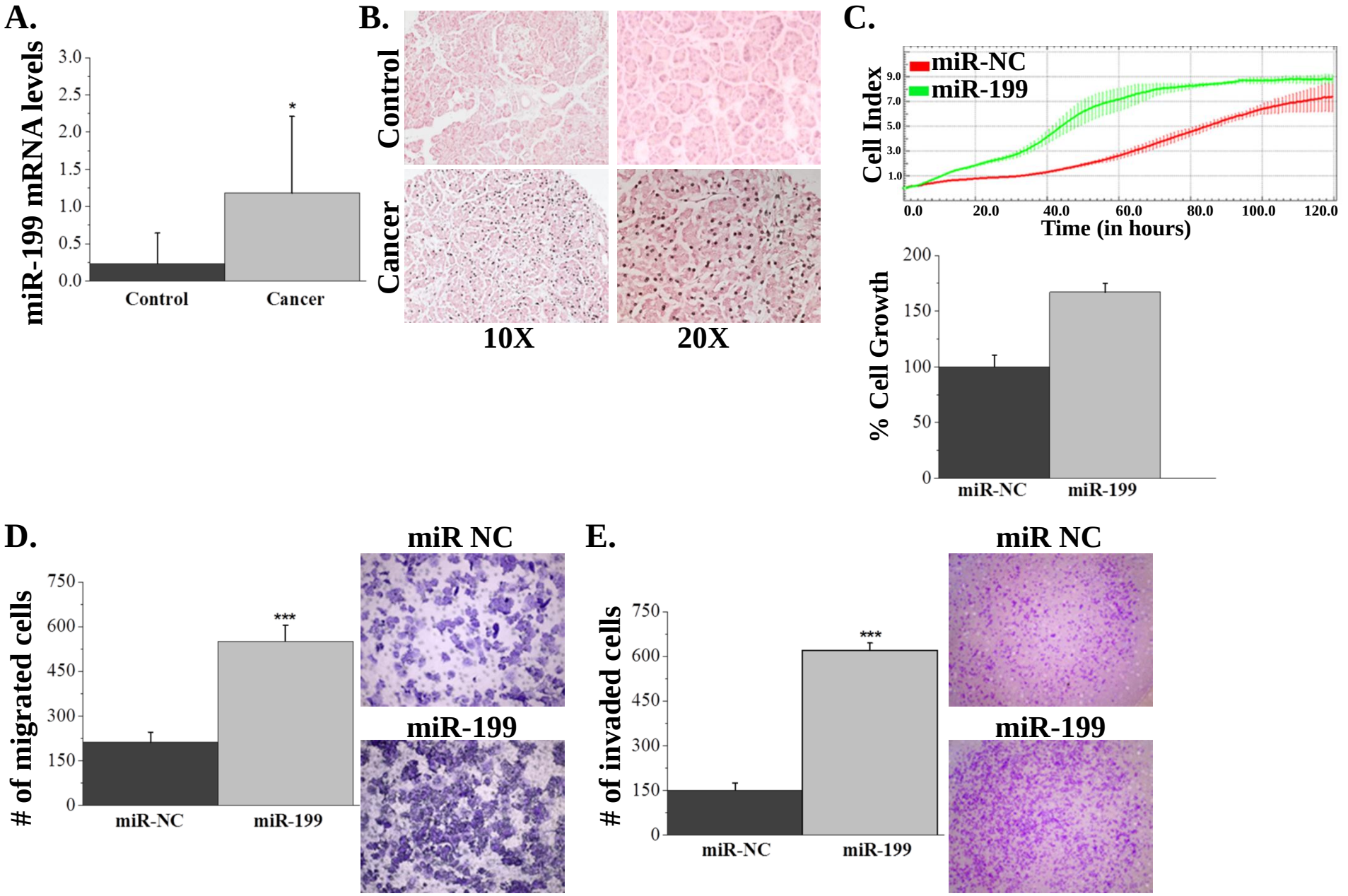
A.
miR-199 mRNA levels
3.0
2.5
2.0
1.5
1.0
0.5
0.0
*
Control
Cancer
B.
Control
Cancer
10X
20X
C.
miR-NC
miR-199
Cell Index
9.0
7.0
5.0
3.0
1.0
0.0
20.0
40.0
60.0
80.0
100.0
120.0
Time (in hours)
% Cell Growth
200
150
100
50
0
miR-NC
miR-199
D.
# of migrated cells
750
600
450
300
150
0
***
miR-NC
miR-199
miR NC
miR-199
E.
# of invaded cells
750
600
450
300
150
0
***
miR-NC
miR-199
miR NC
miR-199

Figure 5

A.

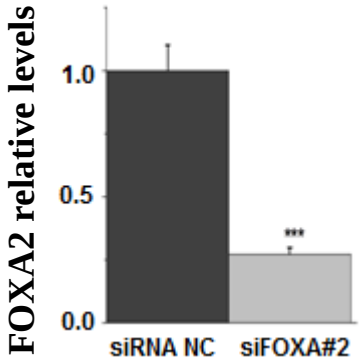

B.

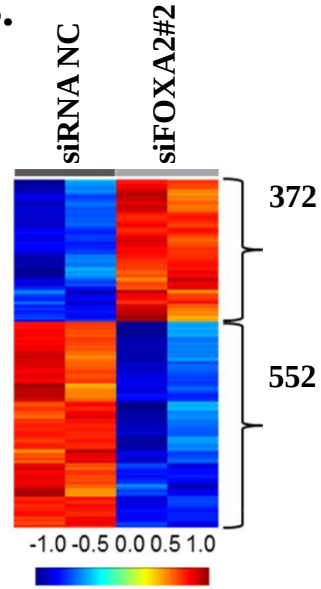

C.

Signaling Pathway	P value
Cell Movement/Invasion	1.28×10^{-5}
Cell Proliferation	4.9×10^{-3}
PI3K/AKT Pathway	1.3×10^{-3}
MAPK Pathway	1.26×10^{-5}

E.

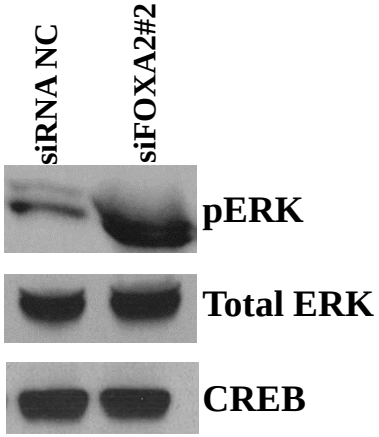

D.

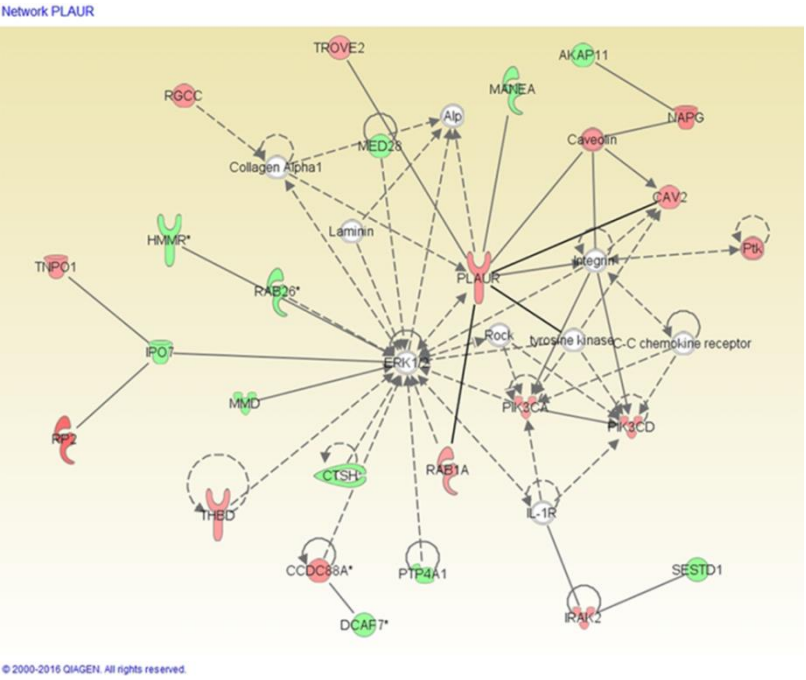

F.

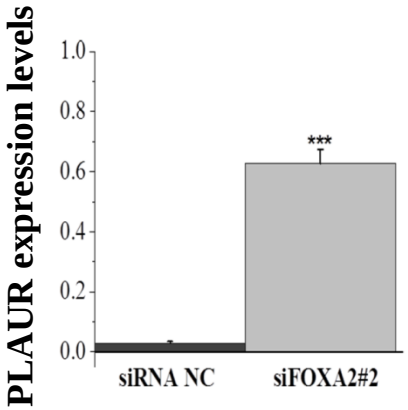

H.

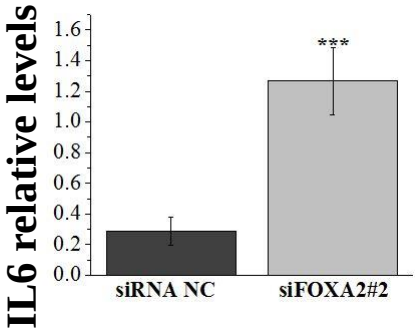

G.

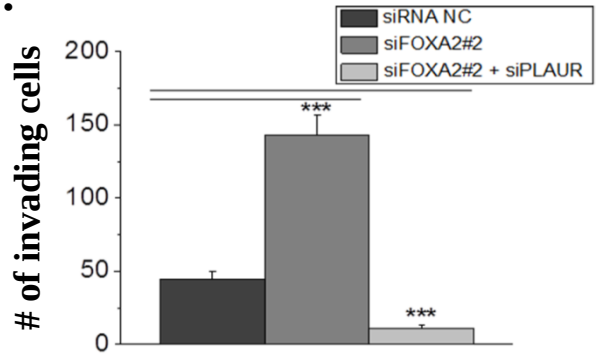

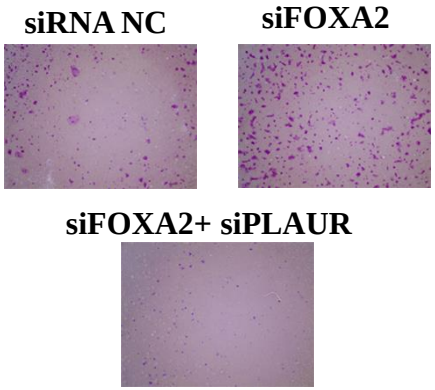

Figure 6

A.

Target Sequence
AAGGGCACGAGCCGTCCGAC

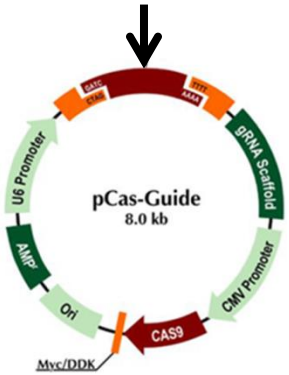

FOXA2 gRNA vector 1

Target Sequence
CACTCGGCTTCCAGTATGCT

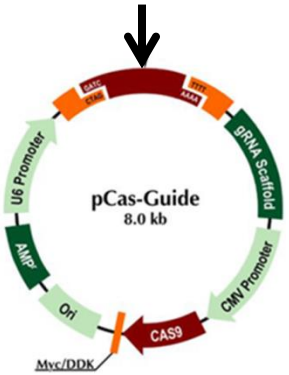

FOXA2 gRNA vector 2

B.

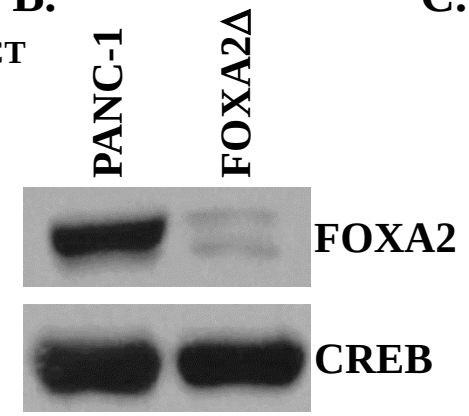

C.

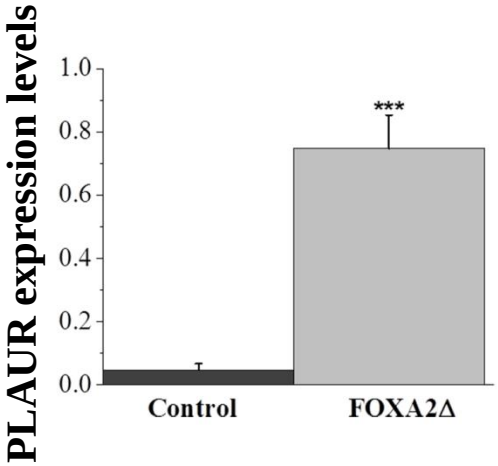

D.

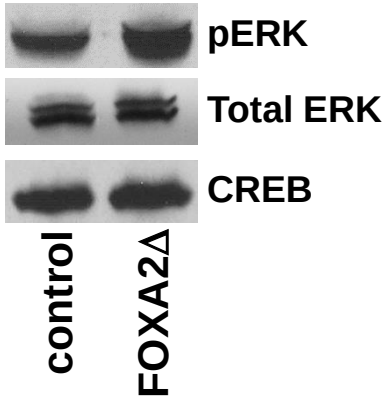

E.

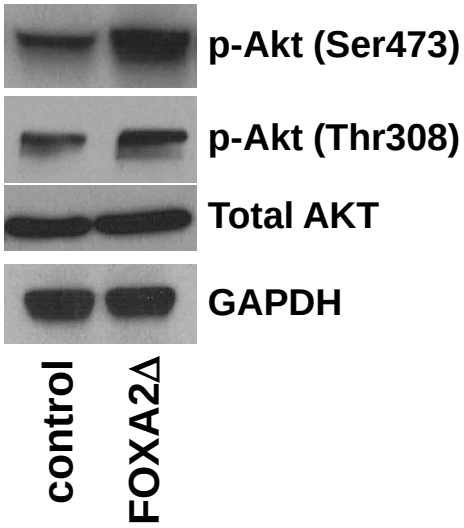

Figure 7

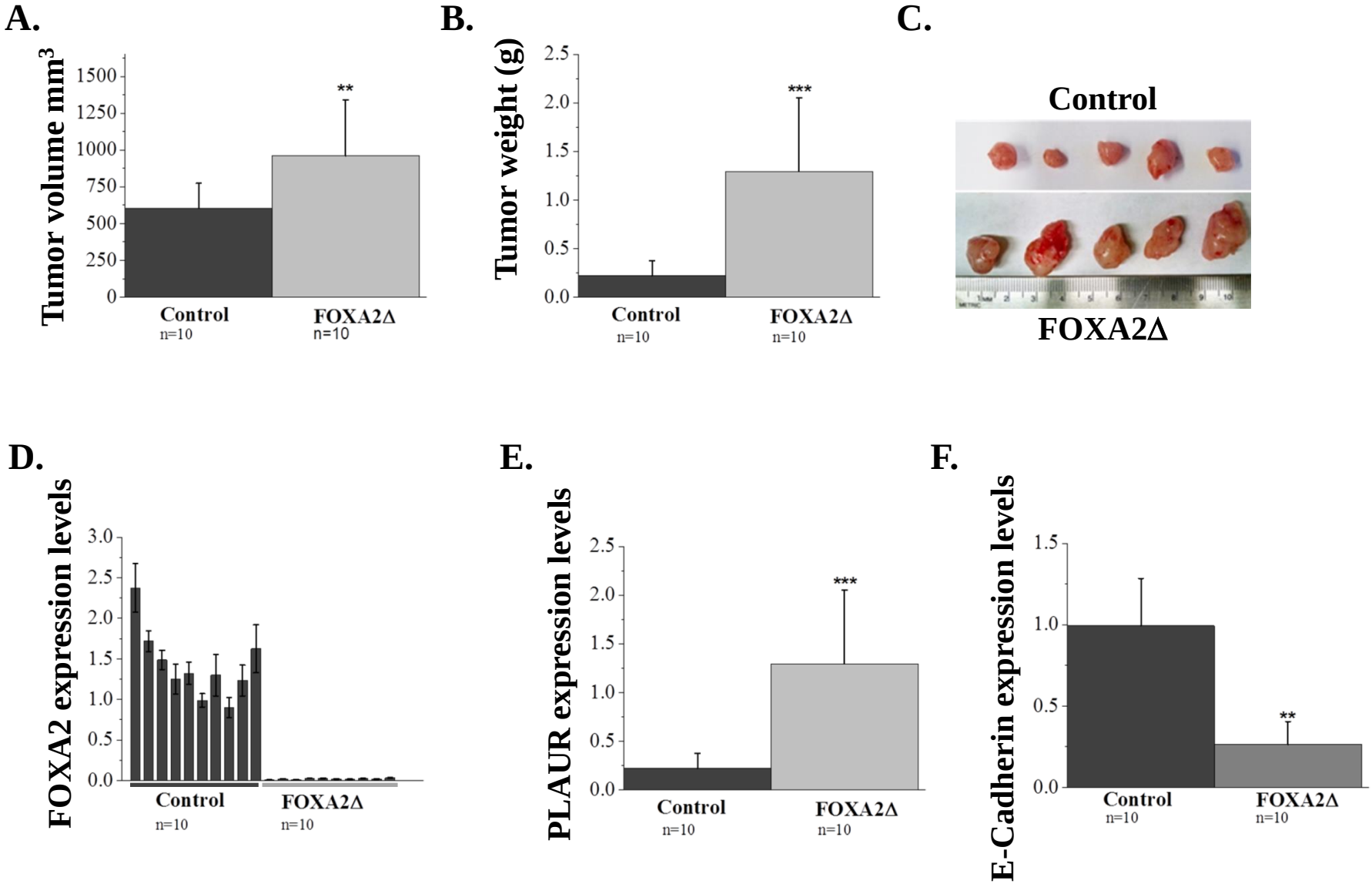
A.
Tumor volume mm3
1500
1250
1000
750
500
250
0
**
Control
n=10
FOXA2Δ
n=10
B.
Tumor weight (g)
2.5
2.0
1.5
1.0
0.5
0.0
***
Control
n=10
FOXA2Δ
n=10
C.
Control
FOXA2Δ
D.
FOXA2 expression levels
3.0
2.5
2.0
1.5
1.0
0.5
0.0
Control
n=10
FOXA2Δ
n=10
E.
PLAUR expression levels
2.5
2.0
1.5
1.0
0.5
0.0
***
Control
n=10
FOXA2Δ
n=10
F.
E-Cadherin expression levels
1.5
1.0
0.5
0.0
**
Control
n=10
FOXA2Δ
n=10

Table 1. Differentially expressed TFs in PDAC vs controls

Transcription Factor Name	Fold Change (PDAC vs Control)
ARNTL2	1.830414193
AHR	1.770715552
BHLHE40	1.620227569
CSDC2	-1.746860866
ELF4	2.026515581
ESRRG	-2.499329116
FOXA2	-1.556944005
FOXF2	1.777107854
FOXL1	1.861434191
FOXP2	-1.520345843
GATA4	-1.824959917
GLIS3	-1.563211851
HHEX	-1.648626826
HMGA2	1.806947596
HNF1B	1.627896229
HOXA3	1.751809197
HOXB2	1.593110965
HOXB6	1.549874116
HOXB7	2.557724696
HOXC9	1.683238922
ID1	1.653506642
KLF15	-2.700062809
KLF4	1.524845007
KLF5	1.728963085
KLF7	1.564062549
LEF1	1.913189882
MAF	1.58038649
MXD1	1.633748967
NR5A2	-3.26744002
ONECUT1	-2.764584396
PDX1	-1.60514131
PPARG	1.802035985
PRDM1	1.995993975
PRDM16	-1.858238085
PRDM5	-1.554285542
PRRX1	1.57618735
PROX1	-2.480756568
SOX6	-1.615514705
TFAP2A	2.652273186
TWIST1	1.921317868
VDR	1.755868703
ZBTB16	-1.687271795